Supporting Information

Spatial and Spectral Super-Resolution Imaging for Characterizing Multichromophoric Systems

*Hyung Jun Kim, Youngah Kwon, Han Yang, Alexander J. Devanny, and Laura J. Kaufman**

Department of Chemistry, Columbia University, New York, New York 10027, United States

*corresponding author: kaufman@chem.columbia.edu

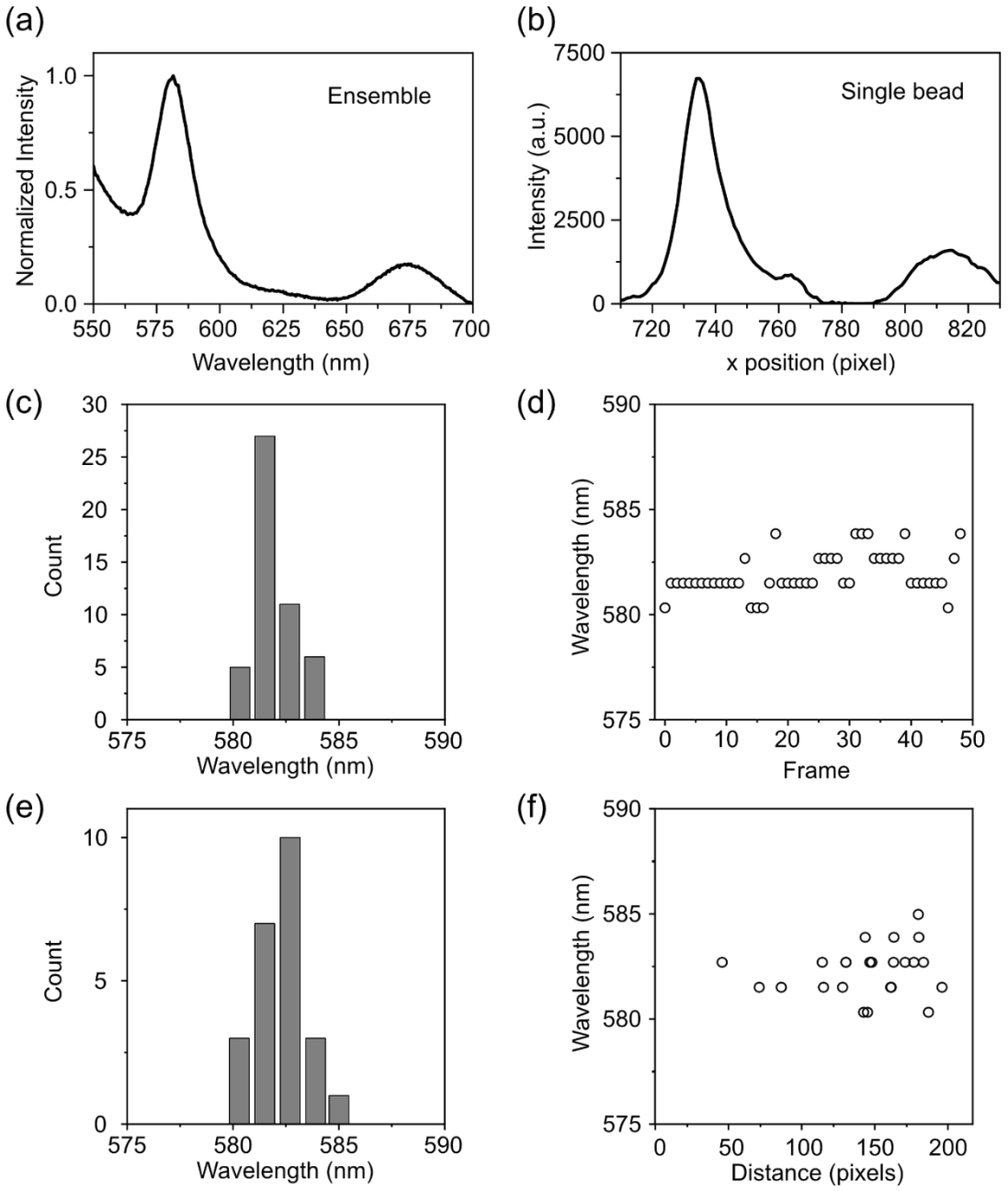

Figure S1. Spectral calibration and precision as obtained from TetraSpeck beads. (a) Emission spectrum of an aqueous TetraSpeck bead solution as measured on a fluorimeter with 405 nm excitation. (b) Line profile versus pixel value in the first-order image obtained from a representative TetraSpeck bead on a coverslip, as collected in the experimental setup shown in Fig. 1 in the main text. Comparison of the peaks leads to Equation 1 in the main text that allows for conversion of pixels to wavelength. (c) Histogram of calibrated maximum peak position of the representative single bead also shown in (b) at each frame (n = 50) in the trajectory. (d) Maximum intensity peak position of this bead vs. frame number. (e) Histogram of maximum peak position over n = 23 beads, each collected over 50 frames. (f) Calibrated maximum peak position of each bead as a function of distance from the imaging center ($\sqrt{\Delta x^2 + \Delta y^2}$) of the zeroth-order image.

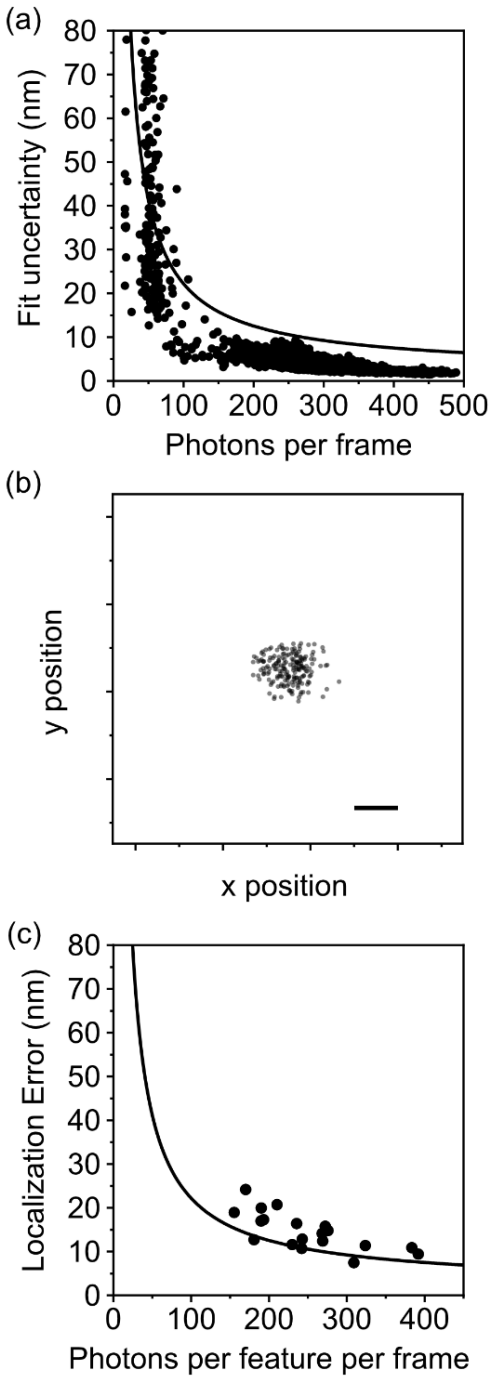

Figures S2. Localization error assessed via measurement of single pPDI molecules. (a) Fit uncertainty as determined by best fits to a 2D Gaussian for each frame collected of the 19 single pPDI molecules (symbols) as well as theoretical prediction (solid line) discussed in the main text. (b) Exemplary localizations for a single pPDI molecule over n = 196 frames. Scale bar = 0.25 pixels (22.5 nm). (c) Localization error as assessed through standard deviation of the localizations such as are shown in (b) as a function of average photon counts from each assessed molecule. Same theoretical result shown in (a) is also shown via the solid line in (c).

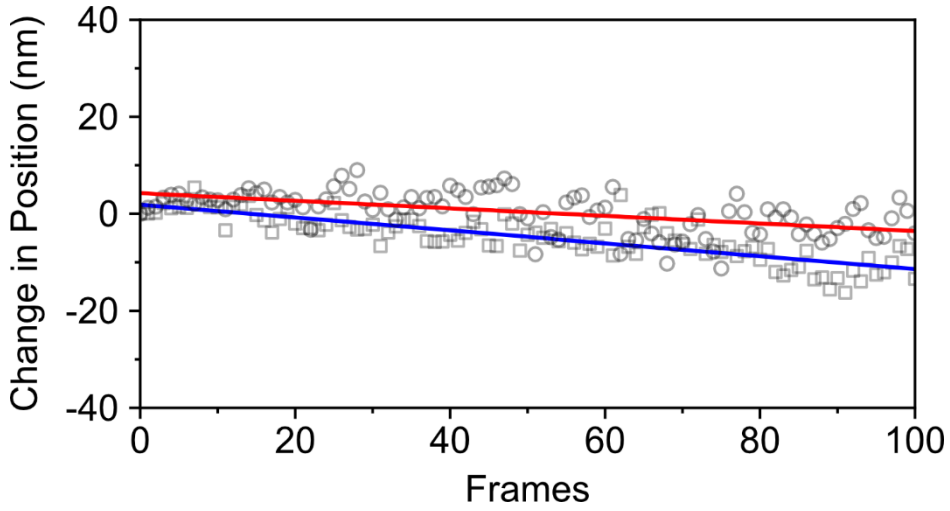

Figure S3. Representative drift assessment from a single movie in which ≈ 120 pPDI features were tracked. Average change in x (circles) and y (squares) position over all features shows drift of < 0.1 nm per frame ≲ 10 nm over the full movie. Red and blue lines are best fit lines to the change in position for x and y positions, respectively. Because SHRImP assessments occur between adjacent frames and (for afSHRImP) frames between adjacent sections, change in position due to drift is comparable to or smaller than localization uncertainty (Fig. S2). As a result, we use movies as collected, which were checked for drift before further assessment. Any movie showing drift above that similar to localization error was not used in further analysis.

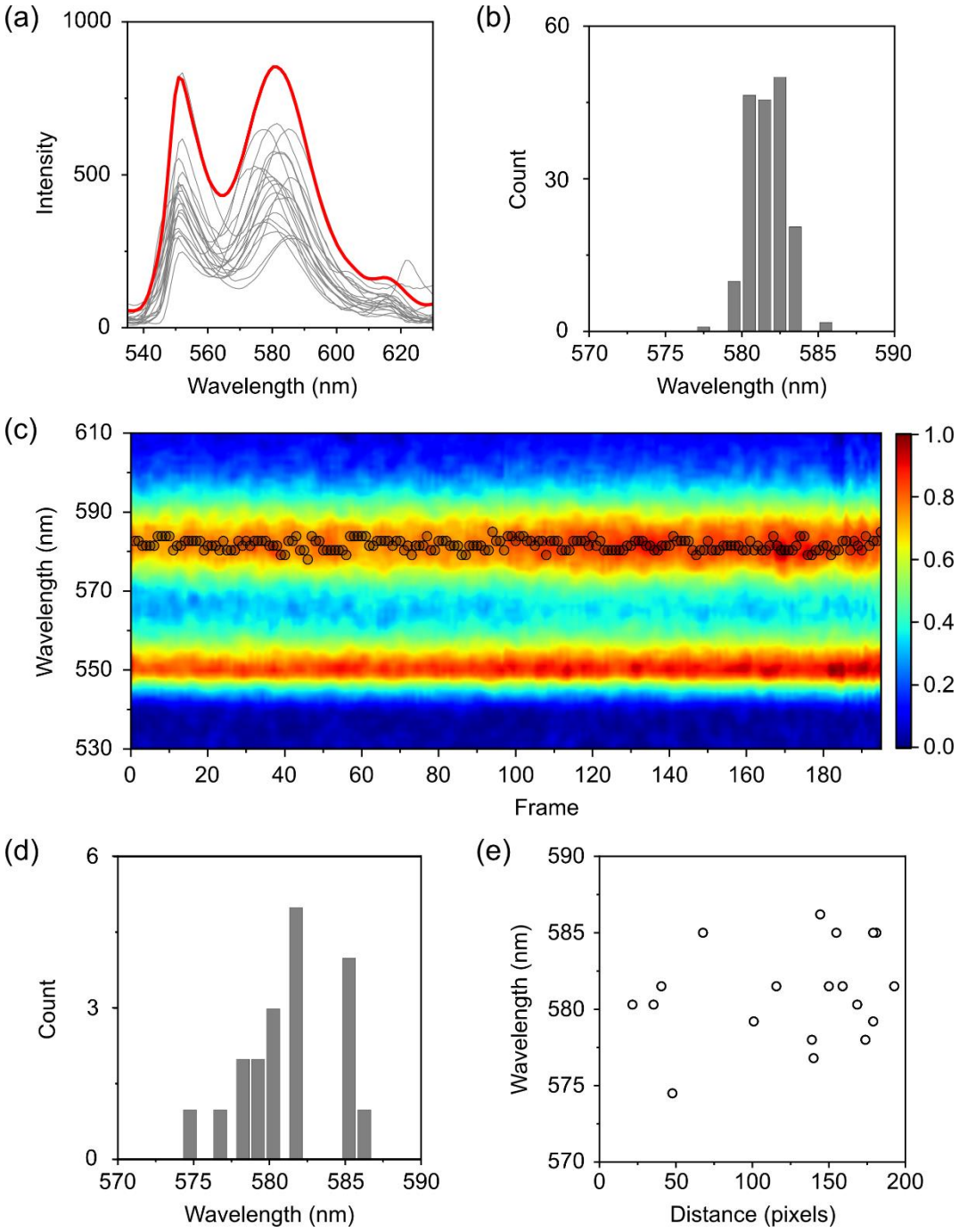

Figure S4. Apparent spectral heterogeneity of single pPDI molecules. (a) Individual (gray) and averaged (red) spectra from the 19 single pPDI molecules also assessed for localization error as shown in Fig. S2. (b) Histogram of maximum 0-1 peak position of the representative pPDI molecule also shown in Fig. S2b at each frame (n = 196) in the trajectory. (c) Stacked spectra of the representative single pPDI molecule over time, with black circles depicting the maximum 0-1 peak positions also shown in (b) over time. The color scale represents normalized intensity. (d) Histogram of maximum peak position of 19 single pPDI molecules, most of which were assessed for 150-200 frames. (e) Maximum peak position of each pPDI molecule as a function of distance from the imaging center of the zeroth-order image.

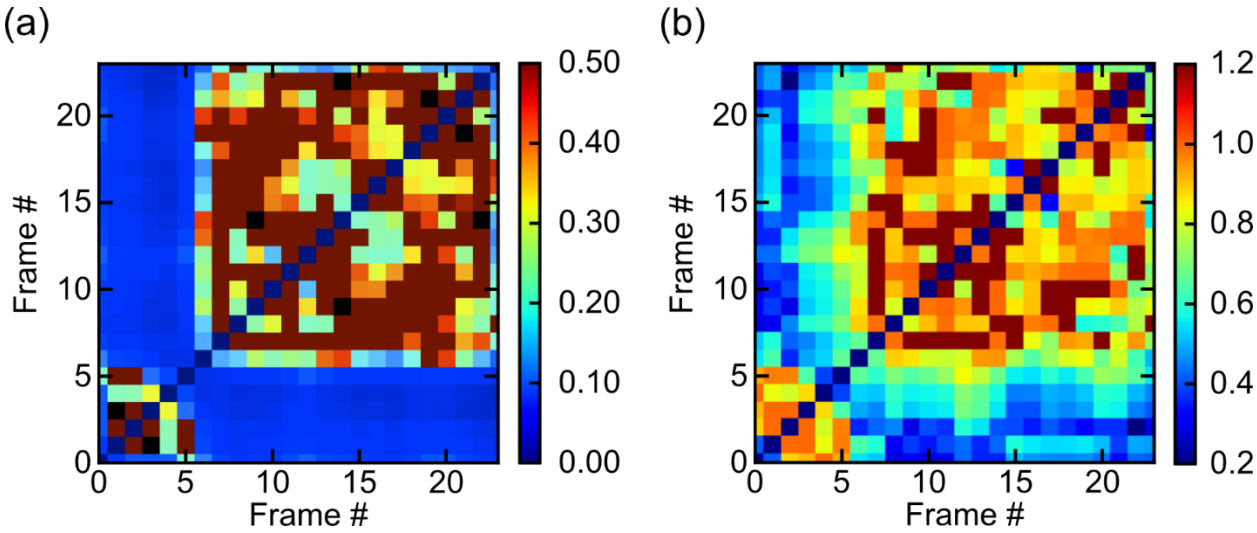

Figure S5. Case study of the same MEH-PPV feature with two emitting sites shown in Fig. 2 of the main text. (a) Two-dimensional contour plot of fit uncertainty of afSHRImP fits. (b) Two-dimensional contour plot of frame-to-frame eccentricity of afSHRImP fits.

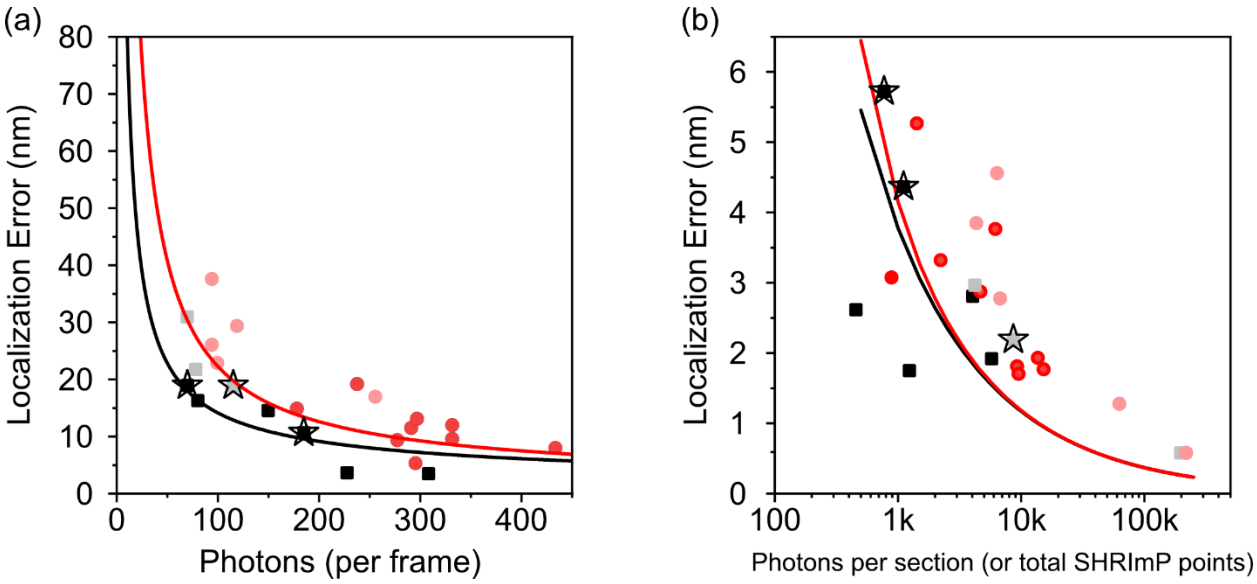

Figure S6. Localization error for MEH-PPV and pPDI features also described in Fig. 2, 4, and 5 in the main text. Points associated with S1, S2, and S2-S1 in Fig. 2 in the main text are shown via stars in this figure. (a) Dark symbols show standard deviation of localizations (as in Fig. S2b) for emitters associated with particular sections of intensity trajectories. Light symbols show equivalent information for positions identified through afSHRImP. Squares represent MEH-PPV and circles pPDI features. Count to photon conversion differs for MEH-PPV and pPDI features because different gain was used in these experiments. Theoretical curves (lines) are also shown: the pPDI curve is the same as that shown in Fig. S2; the MEH-PPV curve uses the same parameters except b = 1.8 photons. (b) Standard error of the mean from averaging with weighted fit uncertainties of the same data shown in (a).

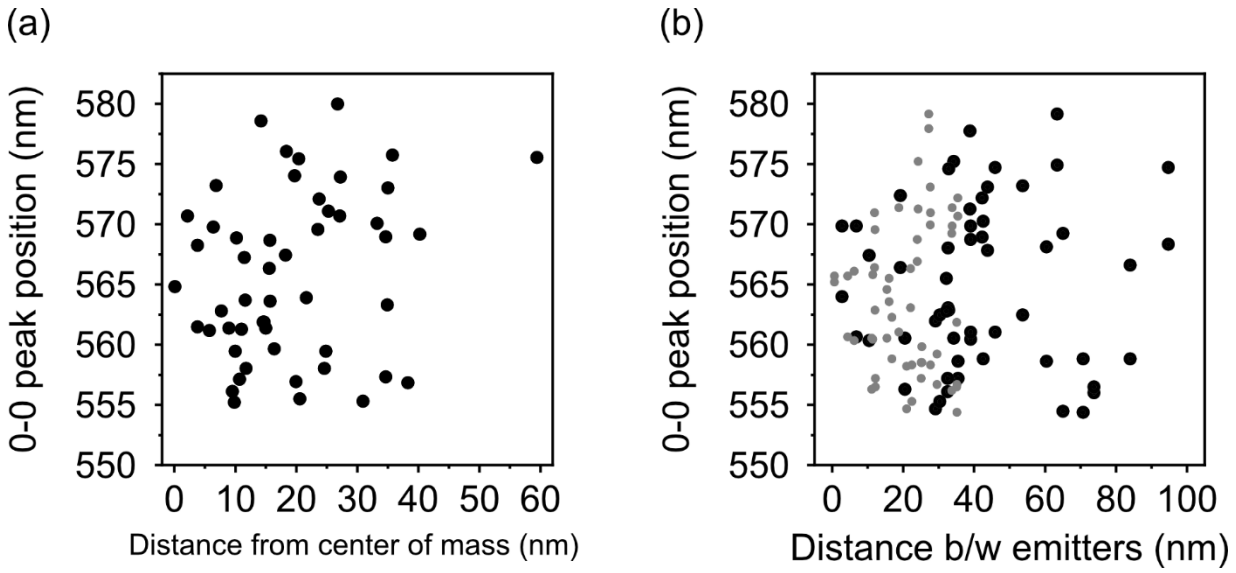

Figure S7. Correlation between spectral and spatial characteristics in MEH-PPV emitters that serially photobleach for the data set also shown in Fig. 3 in the main text. a) Spectral position of the 0-0 peak vs. distance from the center of mass of emission (from the highest intensity section of the intensity trajectory) for each identified emitter. b) Spectral position of the 0-0 peak vs. distance between emitters. In (b) small circles show data from localization imaging and associated sectioned spectra without subtraction while large circles show data following dual spatial and spectral subtractions.

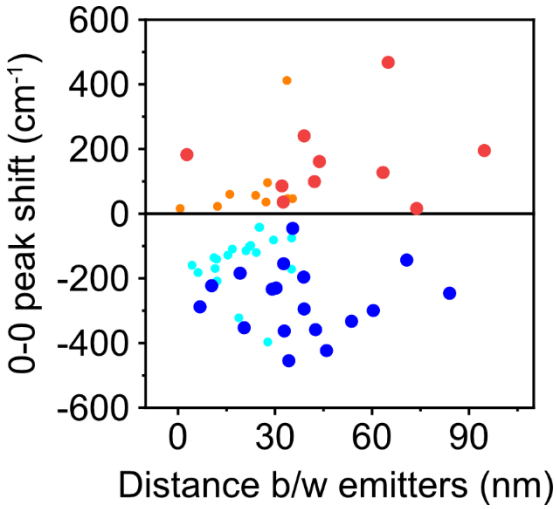

Figure S8. Correlation between spectral and spatial differences in MEH-PPV emitters that serially photobleach for the data set also shown in Fig. 3 in the main text. Shift in spectral position of the 0-0 peak vs. distance between emitters. Small circles show data from localization imaging and associated sectioned spectra without subtraction while large circles show data following dual spatial and spectral subtractions. Red and orange symbols are used for spectra that shift to the red and blue and cyan symbols are used for spectra that shift to the blue after a photobleaching event.

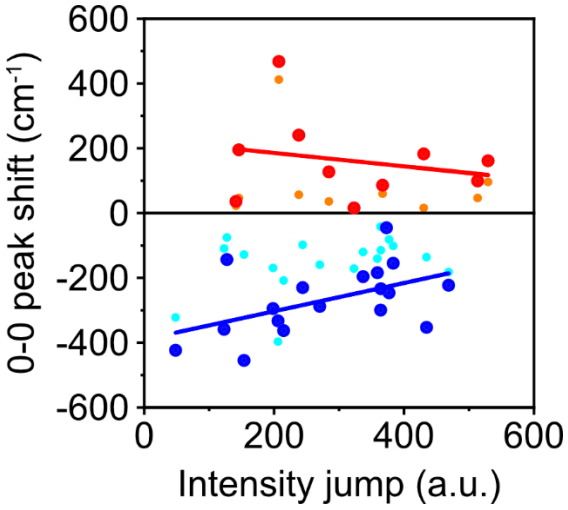

Figure S9. Correlation between spectral shift of the 0-0 peak and intensity change associated with a photobleaching event for MEH-PPV features, with the spectral difference of an emitter relative to the previously photobleached emitter shown as either red (red-shifted) or blue (blue-shifted) points. Large symbols (and best fit lines) are from spectral subtractions. Small cyan and orange symbols are equivalent points obtained from monitoring spectral changes between sections without subtractions. Large symbols and lines are also shown in Fig. 3c in the main text. The best fit line to the small orange symbols (not shown) has a slope of -0.16 and the data has a Pearson's r value of -0.20 while the best fit line to the large red symbols (red line) has a slope of - 0.21 and Pearson's r value of -0.23. Similarly, the best fit line to the small cyan symbols (not shown) had a slope of 0.29 and Pearson's r value of 0.39 while that of the large blue symbols (blue line) had a slope of 0.44 and Pearson's r value of 0.50.

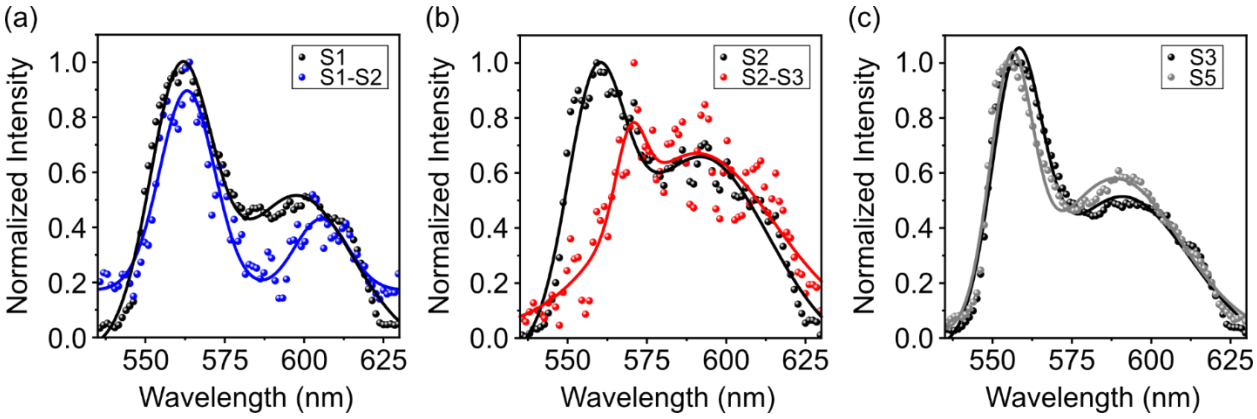

Figure S10. Fluorescence spectra corresponding to the MEH-PPV aggregate with a complex intensity trajectory also shown in Fig. 4 in the main text. The spectra were obtained by averaging all spectra collected during S1 (black in (a)), S2 (black in (b)), S3 (black in (c)), S5 (gray in (c)), and via subtraction (blue in (a) and red in (b)). All spectra or subtraction-generated spectra are normalized. Solid lines represent best fit curves to two Gaussian functions.

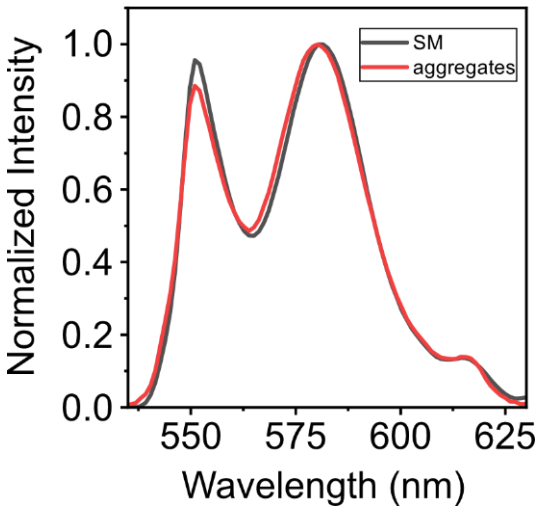

Figure S11. Normalized average spectra of pPDI single molecules (black, also shown in Fig. S4) and pPDI aggregates. n = 19 molecules; n = 16 aggregates.

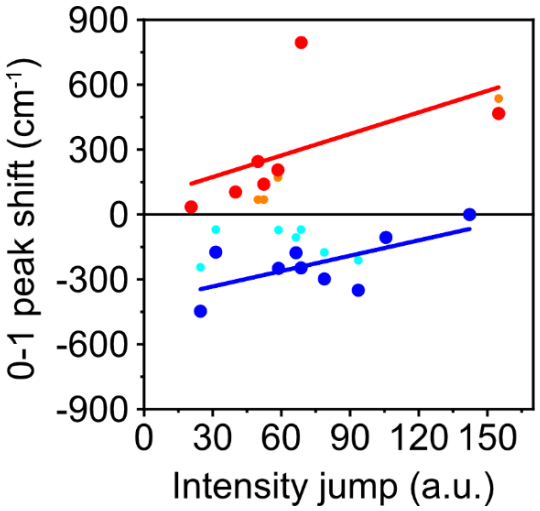

Figure S12. Correlation between spectral shift of the 0-1 peak and intensity change associated with a photobleaching event for a set of 16 pPDI aggregates, with the spectral difference of an emitter relative to the previously photobleached emitter shown as either red (red-shifted) or blue (blue-shifted) points. Large symbols (and best fit lines) are from spectral subtractions. Small cyan and orange symbols are equivalent points obtained from monitoring spectral evolution without subtractions. The best fit line to the small orange symbols (not shown) has a slope of 4.2 and the data has a Pearson's r value of 0.61 while best fit line to the large red symbols (red line) has a slope of 3.32 and Pearson's r value of 0.54. Similarly, the best fit line to the small cyan symbols (not shown) has a slope of 0.89 and Pearson's r value of 0.41 while that of the large blue symbols (blue line) has a slope of 2.38 and Pearson's r value of 0.65.